Quantitative Physiology of Non-Energy-Limited Retentostat Cultures of Saccharomyces cerevisiae at Near-Zero Specific Growth Rates

Liu, Yaya; El Masoudi, Anissa; Pronk, Jack T.; van Gulik, Walter M.

Important note
To cite this publication, please use the final published version (if applicable).
Please check the document version above.

1   **Quantitative physiology of non-energy-limited retentostat cultures of *Saccharomyces***

2   ***cerevisiae* at near-zero specific growth rates**

3   Yaya Liu, Anissa el Masoudi[a], Jack T. Pronk, Walter M. van Gulik[#]

4

5   Department of Biotechnology, Delft University of Technology, Van der Maasweg 9, 2629 HZ

6   Delft, The Netherlands

7

8   # Corresponding author: W.M. van Gulik, e-mail w.m.vangulik@tudelft.nl, telephone

9   +31152784629

10

11   **Key words:** yeast physiology, near-zero growth, retentostat, non-energy limitation, carbon

12   excess

13

14

15

16

17

18

19

20

21

[a] Current address: Royal Haskoning DHV, George Hintzenweg 85, 3009 AM Rotterdam, The

Netherlands.

Abstract:

So far, the physiology of *Saccharomyces cerevisiae* at near-zero growth rates has been studied in retentostat cultures with a growth-limiting supply of the carbon and energy source. Despite its relevance in nature and industry, the near-zero growth physiology of *S. cerevisiae* under conditions where growth is limited by the supply of non-energy substrates remains largely unexplored. This study analyses the physiology of *S. cerevisiae* in aerobic chemostat and retentostat cultures grown under either ammonium or phosphate limitation. To compensate for loss of extracellular nitrogen- or phosphorus-containing compounds, establishing near-zero growth rates ($\mu < 0.002$ h^{-1}) in these retentostats required addition of low concentrations of ammonium or phosphate to reservoir media. In chemostats as well as in retentostats, strongly reduced cellular contents of the growth-limiting element (nitrogen or phosphorus) and high accumulation levels of storage carbohydrates were observed. Even at near-zero growth rates, culture viability in non-energy-limited retentostats remained above 80 % and ATP synthesis was still sufficient to maintain an adequate energy status and keep cells in a metabolic active state. Compared to similar glucose-limited retentostat cultures, the nitrogen- and phosphate-limited cultures showed a partial uncoupling of catabolism and anabolism and aerobic fermentation. The possibility to achieve stable, near-zero growth cultures of *S. cerevisiae* under nitrogen- or phosphorus-limitation offers interesting prospects for high-yield production of bio-based chemicals.

Importance:

The yeast *Saccharomyces cerevisiae* is a commonly used microbial host for production of various bio-chemical compounds. From a physiological perspective, biosynthesis of these compounds competes with biomass formation in terms of carbon and/or energy equivalents. Fermentation processes functioning at extremely low or near-zero growth rates would

46 prevent loss of feedstock to biomass production. Establishing *S. cerevisiae* cultures in which

47 growth is restricted by the limited supply of a non-energy substrate could therefore have a

48 wide range of industrial applications, but remains largely unexplored. In this work we

49 accomplished near-zero growth of *S. cerevisiae* through limited supply of a non-energy

50 nutrient, namely the nitrogen or phosphorus source and carried out a quantitative

51 physiology study of the cells under these conditions. The possibility to achieve near-zero-

52 growth *S. cerevisiae* cultures through limited supply of a non-energy nutrient may offer

53 interesting prospects to develop novel fermentation processes for high-yield production of

54 bio-based chemicals.

55 **Introduction**

56 The yeast *Saccharomyces cerevisiae* is an established microbial host for production of a wide

57 range of bio-chemical compounds (1, 2). Current aerobic processes for production of ATP-

58 requiring ('anabolic') products are typically biphasic, with separate growth and production

59 phases. Complete uncoupling of growth and product formation could enable a further

60 reduction of the loss of feedstock to biomass production. In theory, such a complete

61 uncoupling can be achieved in continuous processes performed at very low or near-zero

62 specific growth rates. In practice, however, its implementation requires processes and

63 microorganisms that, over prolonged periods of time, ensure a high viability and a high

64 biomass-specific product formation rate (q_p) in the absence of growth.

65 For laboratory studies near-zero specific growth rates are usually achieved in retentostats (3).

66 A retentostat is a modification of the chemostat, in which effluent removal occurs through

67 an internal or external filter module that causes complete biomass retention. Retentostats

68 enable studies on microbial physiology at near-zero growth rates that are technically difficult

69 to achieve in conventional chemostats, while their use avoids complete starvation by

70 maintaining a constant supply of essential nutrients.

71 When growth in retentostat cultures is limited by the energy substrate, biomass

72 accumulates in the reactor until the biomass-specific substrate consumption rate (q_s) equals

73 the energy-substrate requirement for cellular maintenance (m_s). Aerobic and anaerobic,

74 glucose-limited retentostat cultures of *S. cerevisiae* were shown to retain a high viability, as

75 well as an extremely high heat-shock tolerance, over periods of several weeks (4-7).

76 Consistent with a growth-rate-independent requirement of ATP for cellular maintenance (8),

77 observed values of q_s at near-zero growth rates ($\mu < 0.002$ h^{-1}) were in good agreement with

78 estimates of m_s derived from measurements in glucose-limited chemostat cultures grown at

79 a range of specific growth rates (4, 6).

80 From an applied perspective, it seems illogical to apply severely energy-limited cultivation

81 regimes for production of compounds whose synthesis from sugar requires a net input of

82 ATP. In nature, *S. cerevisiae* seems to have primarily evolved for growth in sugar-rich

83 environments where, instead of the energy substrate, the nitrogen source is growth limiting

84 (9, 10). Also in industrial substrates for *S. cerevisiae* such as wine most or brewing wort,

85 sugar is typically present in abundance, while growth becomes limited by the nitrogen

86 source (11). As an alternative to nitrogen-limited cultivation, growth under extreme

87 phosphate limitation may offer interesting options to uncouple growth from product

88 formation. For example, *S. cerevisiae,* a non-oleaginous yeast, has been reported to

89 accumulate high levels of specific fatty acids when availability of phosphate is restricted (12).

90 Studies in exponentially growing chemostat cultures have revealed an extensive

91 reprogramming of the yeast transcriptome, proteome and fluxome in response to nitrogen

92 and phosphorus limitation (13-16). In addition, nitrogen- and phosphorus-limited growth of

4

93 resulted in lower contents of protein and phospholipids, respectively, in yeast biomass (17,

94 18). In contrast to the wealth of data on the effects of different nutrient limitation regimes in

95 actively growing cultures, information on aerobic *S. cerevisiae* cultures grown at near-zero

96 growth rates is scarce. In anaerobic cultures, nitrogen-limited cultivation with biomass

97 recycling has been explored to maximize ethanol yields (19, 20). Brandberg and coauthors

98 (21), who investigated the impact of severe nitrogen limitation on ethanol production by *S.*

99 *cerevisiae,* used incomplete cell recycling under anaerobic and micro-aerobic conditions.

100 The goal of the present study is to design and implement retentostat regimes for aerobic,

101 nitrogen- and phosphate-limited growth of *S. cerevisiae* at near-zero specific growth rates

102 and to use the resulting cultures for a first experimental exploration of its quantitative

103 physiology under these scientifically interesting and industrially relevant conditions. To this

104 end, experimental setups were tested that allowed for a smooth transition from low growth

105 rate chemostat cultures to near-zero growth rate retentostat cultures. Metabolic fluxes,

106 biomass composition and cellular robustness were analysed and compared with previously

107 obtained data from glucose-limited chemostat and retentostat cultures.

108 **Results**

109 **Design of carbon-excess retentostat regimes**

110 To study the physiology of *S. cerevisiae* at near-zero growth rates under non-energy-limited

111 conditions, retentostat regimes were designed in which growth was prevented by a severely

112 limited supply of ammonium or phosphate. To avoid starvation, any loss of nitrogen or

113 phosphate from such cultures, either by cell lysis or by excretion of N- or P-containing

114 compounds from viable cells, should be compensated for. As a first approximation of the

115 rates of N and P release by *S. cerevisiae* at near-zero growth rates, concentrations of N- and

116   P-containing compounds were quantified in the outflow of an aerobic, glucose-limited

117   retentostat culture. From these measurements, biomass-specific release rates of 8.1 µmol

118   N/[g biomass]/h and 5.2 µmol P/[g biomass]/h were calculated (Supplementary Table S1).

119   These rates were used to estimate required supply rates of ammonium and phosphate in

120   non-growing retentostat cultures limited by either of these two nutrients. For a target

121   biomass concentration in the retentostats of 5 g/L at a dilution rate of 0.025 h^{-1}, 0.1 g/L

122     $(NH_4)_2SO_4$ was included in the medium feed of the ammonium-limited cultures, while 0.014

123   g/L KH_2PO_4 was used for phosphate-limited retentostat cultivation.

124   Aerobic growth of *S. cerevisiae* at non-limiting concentrations of glucose leads to aerobic

125   alcoholic fermentation (22). Based on trial experiments, glucose concentrations in the

126   influent of ammonium- and phosphate-limited retentostats were set at 120 g/L and 60 g/L,

127   respectively. These concentrations of the growth-limiting nutrients resulted in residual

128   glucose concentrations of ca. 15 g/L. Ethanol concentrations did not exceed 20 g/L, which is

129   well below the value of 5 % (v/v) that has been reported to cause stress responses (23).

130   **Growth and viability in ammonium- and phosphate-limited retentostat cultures**

131   Retentostat cultures were started by redirecting the effluent of steady-state ammonium- or

132   phosphate-limited chemostat cultures, grown at a dilution rate of 0.025 h^{-1}, through a

133   membrane filter unit placed inside the reactor (see Materials and Methods). Replicate

134   ammonium-limited retentostats were operated for 220 h with full biomass retention, after

135   which fouling caused the membrane filters to clog. Membrane fouling was not observed in

136   the phosphate-limited retentostats, which were operated with full biomass retention until,

137   after 400 h, the biomass concentration had reached a stable value.

138   Irrespective of the nutrient limitation regime, the onset of retentostat cultivation led to a

139   gradual increase of the biomass concentration (Fig. 1A and 1B). In ammonium-limited

140   retentostats, the biomass concentration stabilized at ca. 14 g/L after 150 h, while

141   stabilization in the phosphate-limited cultures at ca. 18 g/L occurred after 300 h. The

142   increase in biomass concentration in the ammonium-limited retentostats mainly reflected an

143   increase of the dry mass per cell, which was initially smaller than in the phosphate-limited

144   retentostats. Conversely, the biomass increase in phosphate-limited retentostats

145   predominantly reflected an increase of the cell number (Fig. 1C and 1D).

146   Culture viability was estimated by plate counts of colony-forming units (CFU) and by flow

147   cytometry after CFDA/propidium iodide (PI) staining (Supplementary Table S2). We observed

148   a consistently lower viability in the CFU assays than in the CFDA/PI stains. A similar

149   difference has previously been attributed to loss of viability of retentostat-grown cells during

150   plating (4, 6). Based on PI staining, the viability of the ammonium- and phosphate-limited

151   retentostat cultures towards the end of the experiments did not decrease below 80 % and

152   90 %, respectively (Fig. 1A and 1B, Supplementary Table S2).

153   During retentostat cultivation, specific growth rates progressively decreased, reaching final

154   values of 0.00056 ± 0.00010 h^{-1} and 0.00043 ± 0.00012 h^{-1} for the ammonium- and

155   phosphate-limited cultures, respectively, corresponding to doubling times of 55 and 67 days

156   (Fig. 1E and 1F). Based on these observations, death rates of 0.0018 ± 0.0001 h^{-1} and 0.0012

157   ± 0.0001 h^{-1} were calculated for prolonged ammonium- and phosphate-limited retentostat

158   cultures, respectively. The resulting gradual decrease of culture viability partially explained

159   the difference between the observed biomass accumulation and the targeted values in the

160   experimental design.

Quantitative physiology under extreme ammonium and phosphate limitation

During retentostat cultivation, the biomass-specific consumption rates of glucose and oxygen and production rates of ethanol and CO_2 asymptotically decreased over time and stabilized after approximately 100 h in the ammonium-limited cultures and after approximately 200 h in the phosphate-limited cultures (Supplementary Fig. S1). At this stage, the specific growth rate of the cultures was lower than 0.002 h^{-1}, growth stoichiometries became constant (Fig. 1E and 1F) and cells were assumed to be in a metabolic pseudo steady state. Physiological parameters obtained from the preceding, slowly growing steady-state chemostat cultures (μ = 0.025 h^{-1}) and from the pseudo-steady-state, near-zero growth retentostat cultures (μ < 0.002 h^{-1}) are summarized in Table 1. As anticipated, the concentrations of the limiting nutrients (ammonium or phosphate) were below the detection limit, whereas glucose concentrations were between 10 and 20 g/L in all cultures (Table 1). Carbon- and degree-of-reduction balances yielded recoveries close to 100 % (Table 1), indicating that no major metabolites had been overlooked in the analyses.

In the slow-growing (μ = 0.025 h^{-1}) chemostat cultures the biomass-specific rates of glucose and oxygen consumption as well as ethanol and carbon dioxide production, were consistently higher in the phosphate-limited cultures than in the ammonium-limited cultures (Table 1). In line with these observations, the phosphate-limited cultures showed a lower biomass yield and higher ethanol yield on glucose. Respiratory quotients (RQ, ratio of CO_2 production and O_2 consumption rate) were identical for the two nutrient limitation regimes, indicating that the difference in biomass yield of the chemostat cultures was not caused by different contributions of respiratory and fermentative metabolism. Furthermore, the sum of the specific production rates of the four minor byproducts (glycerol, succinate, lactate and acetate), which accounted for less than 4 % of the consumed glucose, were not significantly

8

185   different for the two limitation regimes and were also not responsible for the observed

186   difference in biomass yield.

187   In the pseudo-steady-state near-zero growth retentostat cultures, the observed ethanol

188   yields on glucose (Table1) were respectively 71 % and 53 % of the theoretical maximum

189   (0.51 g ethanol/[g glucose]) for the ammonium- and phosphate-limited regimes. Consistent

190   with this observation, significant oxygen consumption occurred in these cultures and their

191   RQ values were significantly lower than those of the preceding chemostat cultures. For the

192   phosphate-limited cultures the difference was most pronounced. These observations

193   indicate that near-zero growth achieved by phosphate limitation leads to a more respiratory

194   metabolism than was observed in the preceding slowly growing, phosphate-limited

195   chemostats. Formation of byproducts accounted for 16 % and 11 % of the supplied glucose

196   in the ammonium- and phosphate-limited near-zero growth cultures, respectively. Glycerol

197   and succinate were the main contributors, with succinate accounting for 9 % of the

198   consumed glucose in the ammonium-limited culture.

199   **Biomass composition under extreme ammonium and phosphate limitation**

200   To analyse the impact of extreme ammonium and phosphate limitation on biomass

201   composition, biomass samples from slow growing, steady-state chemostat cultures and from

202   near-zero growth rate pseudo-steady-state retentostat cultures were analysed for their

203   elemental and macromolecular compositions (Table 2). In the chemostat cultures as well as

204   in the retentostat cultures, the content of the growth-limiting element in the biomass was

205   strongly reduced relative to that of the culture grown under the other nutrient limitation

206   (Table 2). This difference was even more pronounced in the retentostat cultures than in the

207   preceding chemostat cultures. The nitrogen content of biomass from ammonium-limited

208 retentostat cultures was ca. 2-fold lower than that of the corresponding phosphate-limited

209 retentostats, while the phosphorus content of biomass from the phosphate-limited

210 retentostats was 3.5-fold lower than that of biomass from the ammonium-limited

211 retentostats. Both in phosphate-limited chemostats and retentostats, a low phosphorus

212 content was accompanied by a 2-3 fold higher sulfur content than in the corresponding

213 ammonium-limited cultures. The increased sulfur content in phosphate-limited cultures may

214 be due to sulfate uptake by high-affinity phosphate transporters (14). Compared with

215 glucose-limited chemostat cultures of the same *S. cerevisiae* strain at a similar dilution rate

216 (D= 0.022 h^{-1}, Table 2), the biomass protein content and the total nitrogen content of cells

217 grown in the ammonium-limited chemostat cultures were over 60 % and 50 % lower,

218 respectively. Similarly, in the phosphate-limited chemostat cultures, the phosphorus

219 content of the biomass was ca. 50 % lower.

220 Consistent with their low nitrogen content, ammonium-limited chemostat and retentostat

221 cultures showed a ca. 2.5-fold lower biomass protein content than the corresponding

222 phosphate-limited cultures, with the lowest protein content (9.6 %) measured in the

223 ammonium-limited retentostats (Fig. 2A). Conversely, glycogen contents were higher (5.8

224 fold in chemostats and 1.8 fold in retentostats) in ammonium-limited cultures than in

225 phosphate-limited cultures, while trehalose contents were only 30-40 % higher in the

226 ammonium-limited cultures (Fig. 2B). When analysed throughout the retentostat

227 experiments, glycogen contents in the ammonium-limited cultures remained consistently

228 high, while they increased with declining specific growth rate in the phosphate-limited

229 cultures (Fig. 2C). For both nutrient limitation regimes, the trehalose content reached a

230 maximum at a specific growth rate of ca. 0.01 h^{-1} (Fig. 2D).

Metabolic flux analysis

To further investigate the physiological differences between extreme ammonium and phosphate limitation, metabolic flux analysis was performed for both the slow growing, steady-state chemostat cultures ($\mu = 0.025$ h^{-1}) and near-zero growth, pseudo-steady-state retentostat cultures ($\mu < 0.002$ h^{-1}) (Fig. 3, Supplementary Table S3). At a specific growth rate of 0.025 h^{-1}, fluxes through the glycolysis, tricarboxylic acid cycle (TCA cycle) and pyruvate branch point were consistently higher in the phosphate-limited cultures than in the ammonium-limited cultures. This observation indicated a higher contribution of catabolism in the phosphate-limited cultures. Assuming a P/O ratio of 1 (24), biomass-specific rates of ATP turnover were ca. 1.3-folder higher in the phosphate-limitated chemostat cultures than in the corresponding ammonium-limited cultures (Fig. 3).

In the retentostats, fluxes through the pentose-phosphate pathway (PPP) were extremely low, which is consistent with the strictly assimilatory role of this central metabolic pathway in *S. cerevisiae* (25). The glycolytic flux was nearly identical for the two nutrient limitations. Conversely, distribution of pyruvate over alcoholic fermentation and TCA cycle were different. Consistent with their lower RQ, phosphate-limited retentostat cultures channeled a higher fraction of the pyruvate into the TCA cycle than the ammonium limited retentostat cultures. Estimated non-growth-associated ATP consumption was higher in the phosphate-limited retentostats (3.4 ± 0.2 mmol ATP/[g viable biomass]/h) than in the ammonium-limited retentostats (2.9 ± 0.1 mmol ATP/[g viable biomass]/h) (Fig. 3).

Energetics under extreme ammonium and phosphate limitation

Nitrogen and phosphate limitation can both be characterized as non-energy-limited cultivation regimes. However, because phosphate plays a vital role in cellular energy

11

254 metabolism and energy status, the intracellular nucleotide levels (ATP, ADP and AMP) and

255 corresponding adenylate energy charge and ATP/ADP ratios were quantified for both

256 chemostat and retentostat conditions (Fig. 4). Intracellular levels of all three adenine

257 nucleotides were consistently higher in the chemostats than in the retentostats. Comparing

258 these two limitations, both in slow-growth and near-zero growth cultures, intracellular ATP

259 and AMP levels were consistently lower under phosphate limitation than under ammonium

260 limitation. In addition, phosphate-limited near-zero growth cultures also showed ca. 40 %

261 lower ADP levels than the corresponding ammonium-limited cultures, while ADP levels were

262 identical in phosphate- and ammonium-limited, slow-growing chemostat cultures (Fig. 4A).

263 Neither the ATP/ADP ratios nor the energy charge in the retentostat cultures differed from

264 those in the corresponding slow-growing chemostat cultures (Fig. 4B and 4C). However,

265 ATP/ADP ratios in the phosphate-limited cultures were 30–35 % lower than in the

266 corresponding ammonium-limited cultures. A similar, less pronounced difference was

267 observed for the adenylate energy charge. These results show that phosphate limitation

268 indeed significantly affected cellular energy status.

269 **Discussion**

270 **Prolonged near-zero growth of *S. cerevisiae* under non-energy-limited conditions**

271 Retentostat cultivation of heterotrophic microorganisms typically involves a constant,

272 growth-limiting supply rate of the carbon and energy substrate (3). The amount of viable

273 biomass in such energy-limited retentostats asymptotically increases to a constant value,

274 while the specific growth rate asymptotically approaches zero. In the resulting pseudo

275 steady states, biomass-specific substrate supply rates closely match cellular maintenance-

276 energy requirements (3). The retentostat regimes explored in this study, in which growth

277 was restricted by supply of the nitrogen or phosphorus source, represented a fundamentally

278 different scenario. While biomass also asymptotically increased to a constant value, the

279 corresponding constant biomass-specific ammonium or phosphate consumption rates were

280 not related to maintenance-energy metabolism. Instead, they represented release of

281 nitrogen- or phosphorus-containing compounds, which were removed via the cell-free

282 effluent.

283 Excretion of nitrogen- or phosphorus-containing compounds by severely ammonium- or

284 phosphate-limited yeast cultures appears counter intuitive. Instead, release of these

285 compounds probably occurs by cell death and/or lysis. *S. cerevisiae* can express a range of

286 specific and non-specific amino acid permeases (26), while di- and tri-peptides can be

287 imported by Prt2p (27). Presence of amino acids in culture supernatants is therefore likely to

288 reflect the kinetics of such transporters, rather than a complete inability for amino-acid

289 reconsumption by viable cells. Consistent with this hypothesis, extracellular concentrations

290 of amino acids in the ammonium-limited retentostats were lower than the K_m values of the

291 corresponding high-affinity *S. cerevisiae* amino-acid permeases (Supplementary Table S4).

292 Biomass concentrations in the ammonium- and phosphate-limited retentostats reached

293 values that were approximately 3-fold higher than the target value of 5 g/L on which design

294 of growth media and operating conditions were based. This difference could only partially be

295 attributed to accumulation of non-viable biomass. In addition, strongly reduced contents of

296 the growth limiting element in the retentostat-grown biomass could explain this large

297 discrepancy to a large extent.

298 As previously reported for glucose-limited cultures (21), ammonium- and phosphate-limited

299 cultivation of *S. cerevisiae* at low to near-zero growth rates led to increased intracellular

300 levels of glycogen and trehalose. This observation confirms that glycogen and trehalose

301 accumulation is a universal physiological response of *S. cerevisiae* at near-zero growth

302 conditions. Also in faster growing chemostat cultures, nitrogen limitation has been shown to

303 lead to higher storage carbohydrate levels than other nutrient-limitation regimes (28).

304 Intracellular reserves of glycogen and trehalose enable survival during carbon and energy

305 source starvation and can fuel cell cycle progression under carbon- and energy-source

306 limitation (29). Additionally, upregulation of genes involved in synthesis, metabolism and

307 degradation of trehalose has been implicated in the extreme heat-shock tolerance of

308 glucose-limited retentostat cultures of *S. cerevisiae* (6, 30).

309 **Energy metabolism of *S. cerevisiae* under extreme ammonium and phosphate**

310 **limitation**

311 Despite strongly reduced phosphate content and low intracellular levels of adenosine

312 nucleotides, the adenylate energy charge of 0.83 of the phosphate-limited chemostat and

313 retentostat cultures was within the normal physiological range of 0.7 to 0.95 (31)*. Also the

314 adenylate energy charge of 0.88 for the corresponding ammonium-limited cultures indicated

315 that cells were able to maintain their energy status under extreme nutrient restriction.

316 Consistent with the well-known tendency of *S. cerevisiae* to exhibit aerobic alcoholic

317 fermentation when exposed to excess glucose (22), respiratory quotients (RQs) of all

318 ammonium- and phosphate-limited cultures were above 1. RQ values were lowest at near-

319 zero growth rates (Supplementary Table S5), indicating that the contribution of fermentative

320 metabolism decreased with decreasing specific growth rate. Even though *S. cerevisiae* has a

321 low P/O ratio, respiratory catabolism of glucose yields much more ATP than fermentation

322 (32). However, it maximum rate of fermentative ATP generation is approximately 2-fold

323 higher than its maximum rate of respiratory ATP generation (33). These observations

324 underlie a rate/yield trade-off hypothesis, according to which ATP can either be produced

325 fast (but with a low efficiency) or efficiently (but at a lower maximum rate) (34). The shift

326 towards a more respiratory metabolism in the near-zero growth rate retentostat cultures is

327 entirely in line with this hypothesis.

328 Non-growth associated rates of ATP turnover in the aerobic, non-energy-limited cultures

329 were significantly higher than maintenance-energy requirements estimated from aerobic

330 and anaerobic energy-limited retentostat studies with the same *S. cerevisiae* strain

331 (supplementary Fig. S3). While a similar uncoupling of anabolic energy demand and catabolic

332 energy conservation has been reported for nitrogen-limited chemostat cultures, the

333 underlying mechanism has not been elucidated (16, 21, 35-38). Quantification of the *in vivo*

334 cytosolic concentrations of ammonium and ammonia recently showed that, in ammonium-

335 limited chemostat cultures of *S. cerevisiae* grown at pH 5, cytosolic ammonia concentrations

336 exceeded extracellular concentrations (39). Diffusion of ammonia from the cells, combined

337 with reuptake of ammonium cation by the high-affinity uniporter Mep2 (40) and expulsion

338 of its associated proton by the plasma-membrane H^+-ATPase Pma1 could lead to a futile

339 cycle.

340 Extreme phosphate-limited growth of *S. cerevisiae* induces expression of *PHO84*, which

341 encodes a high-affinity phosphate/proton symporter and vacuolar synthesis of inorganic

342 polyphosphate(41). By acting as a phosphorus sink, polyphosphate sustains phosphate

343 uptake at low extracellular concentrations (41, 42). Its synthesis in yeast requires activity of

344 the vacuolar H^+-ATPase (V-ATPase) to maintain a proton-motive force across the vacuolar

345 membrane (41). Although high-affinity phosphate import and subsequent vacuolar

346 polyphosphate synthesis must have resulted in increased ATP requirements, these are

347 negligible compared to the observed non-growth associated ATP requirements in the

348   phosphate-limited retentostat cultures. Unless very significant turnover of the

349   polyphosphate pool has occurred, these additional ATP requirements are likely to have been

350   caused by other, yet unknown processes.

Possible application of severe ammonium or phosphate limitation for industrial processes

353   Metabolic engineering of *S. cerevisiae* has enabled the production of a wide range of

354   compounds whose biosynthesis from sugars requires a net input of ATP (43). The specific

355   rate of formation of such 'anabolic' products is determined by the capacities and regulation

356   of the enzymes of the product pathway and connected primary metabolic pathways, as well

357   as by the continuous (re)generation of cofactors such as NAD(P)H, Coenzyme A and ATP. To

358   optimize yields of such products, allocation of sugar to growth should be minimized. At the

359   same time, ATP availability should not limit product formation rates. Theoretically, these

360   goals can be reconciled by near-zero-growth-rate cultivation under non-energy-limited

361   conditions. This study shows that, under ammonium limitation as well as under phosphate

362   limitation, glucose-sufficient, near-zero-growth retentostat cultures of a laboratory strain of

363   *S. cerevisiae* is able to maintain a normal energy charge and showed only a modest loss of

364   culture viability. The extremely low protein content of biomass grown in the nitrogen-limited

365   retentostats is likely to represent a disadvantage for high-level expression of heterologous

366   product pathways. Moreover, nitrogen limitation is intrinsically poorly suited for production

367   of proteins and other nitrogen-containing compounds. Extreme phosphate limitation did not

368   affect biomass protein levels. However, relative to glucose-limited retentostats, both the

369   ammonium- and phosphate-limited cultures showed increased rates of non-growth

370   associated ATP dissipation. This increase is undesirable in industrial contexts, as the resulting

16

371   increased rate of sugar dissimilation would go at the expense of the product yield. Future

372   research should therefore aim at identifying the causes of non-growth associated ATP

373   dissipation and on their elimination, either by alternative nutrient limitation regimes, by

374   strain engineering or by alternative approaches to restrict cell division.

375   **Materials and methods**

376   ## Yeast strain and media

377   The prototrophic, haploid yeast strain *Saccharomyces cerevisiae* CENPK 113-7D was used in

378   this study (44). Working stocks were obtained by cultivation in YPD medium (10 g/L Bacto

379   yeast extract, 20 g/L Bacto peptone and 20 g/L D-glucose). After addition of 30 % (v/v)

380   glycerol, culture aliquots were stored in sterilized Eppendorf tubes at -80°C.

381   Ammonium- and phosphate-limited (N- and P-limited) pre-culture and batch culture media

382   were prepared as described by Boer (16). For N-limited batch cultivation, the medium

383   contained the following components: 1.0 g of $(NH_4)_2SO_4$, 5.3 g of K_2SO_4, 3.0 g of KH_2PO_4, 0.5

384   g of $MgSO_4\_7H_2O$, and 59 g of glucose per liter. For P-limited batch cultivation, the medium

385   contained 5.0 g of $(NH_4)2SO_4$, 1.9 g of K_2SO_4, 0.12 g of KH_2PO_4, 0.5 g of $MgSO_4\_7H_2O$, and 59

386   g of glucose per liter. In addition, 1 mL/L trace element solution ,1 mL/L vitamin solution

387   and 0.2 g/L Pluronic 6100 PE antifoaming agent (BASF, Ludwigshafen, Germany) were added.

388   Trace element and vitamin solutions were prepared as described by Verduyn (45). The

389   compositions of media for N- and P-limited chemostat cultivation were as described above,

390   except that the glucose concentration was increased to 120 g/L. For N-limited retentostat

391   cultivation, the $(NH_4)_2SO_4$ concentration in the medium feed was decreased to 0.1 g/L and

392   the glucose concentration was 60 g/L. To maintain the same sulfur concentration, the K_2SO_4

393   concentration was increased to 6.46 g/L, the concentrations of the other compounds were

394 the same as in the chemostat medium. For P-limited retentostat cultivation, the KH_2PO_4

395 concentration was lowered to 0.014 g/L and the glucose concentration was 60 g/L.

Bioreactor set up

397 Bench-scale, turbine-stirred 7 L bioreactors (Applikon, Delft, The Netherlands) equipped

398 with a single six-bladed Rushton turbine impeller with a diameter of 85 mm, were used in

399 this study. The working volume was controlled at 5 L by placing the bioreactor on an

400 electronic balance (Mettler Toledo, Columbus, Ohio, USA). During continuous cultivation,

401 effluent was removed with a peristaltic pump to an effluent vessel, which was placed on an

402 electronic balance for measurement of the dilution rate ($D = 0.025$ h^{-1}). The culture

403 temperature was maintained at $30 \pm 0.1^{o}C$ and the stirrer speed at 500 rpm. Aerobic

404 conditions were maintained by sparging 0.5 vvm compressed air, controlled by a mass flow

405 controller (Brooks 5850 TR, Hatfield, PA, USA). The dissolved oxygen concentration was

406 measured on-line with a DO sensor (Mettler-Toledo GmbH, Greinfensee, Switzerland) and

407 remained above 30 % of air saturation in all experiments. Culture pH was controlled at 5.00 ±

408 0.05 by automated addition of either 2 M KOH or 2 M H_2SO_4, using a Biostat Bplus controller

409 (Sartorius BBI Systems, Melsungen, Germany). Exhaust gas was cooled to 4°C by an in-line

410 condenser and dried by a Nafion dryer (Permapure, Toms River, USA) before entering a

411 combined paramagnetic/infrared NGA 2000 off-gas analyzer (Rosemount Analytical,

412 Anaheim, USA) for analysis of O_2 and CO_2 concentrations. Off-gas data were acquired with

413 MFCS/win 3.0 software (Sartorius BBI Systems, Melsungen, Germany).

Pre-culture, batch, chemostat and retentostat cultures

415 Pre-cultures, grown in 500 mL shake flasks containing 200 mL medium, were inoculated with

416 2 mL of stock culture and grown at 30°C and at 200 rpm for 8 h in a B Braun Certomat BS-1

417   incubator (Sartorius, Melsungen, Germany). Bioreactor batch cultures were started by

418   transferring 400 mL of preculture to a bioreactor containing 4.6 L of medium. After

419   approximately 24 h of batch cultivation, a sharp decrease of the CO_2 concentration in the

420   off-gas and a corresponding increase of the dissolved oxygen concentration indicated that

421   ammonium or phosphate was depleted. The bioreactors were then switched to chemostat

422   cultivation mode and operated at a dilution rate of 0.025 h^{-1}. Steady-state was assumed to

423   be achieved after 5 volume changes, in which stable (less than 3 % difference over 2 volume

424   changes) off-gas CO_2 and O_2 concentrations, culture dry weight and cell counts were

425   observed. At that stage, bioreactors were switched from chemostat to retentostat mode by

426   redirecting the culture effluent through a filtration probe assembly (Applikon, Delft, The

427   Netherlands). Each probe was fitted with a 0.22 μm tubular micro-filtration polypropylene

428   membrane (TRACE Analytics, Brunswick, Germany). Because of the limited flow rate capacity

429   of each filter, four filtration probes were installed in each bioreactor. Before mounting on

430   the filtration probe and autoclaving, membranes were hydrophilized overnight in 70 % (v/v)

431   isopropanol.

432   To avoid a sudden decrease of substrate concentrations during the switch from chemostat

433   to retentostat mode, a gradual transition from chemostat to retentostat medium was

434   accomplished by using two feed pumps. The resulting time-dependent concentrations of

435   glucose and of the growth-limiting nutrient ($(NH_4)_2SO_4$ or KH_2PO_4) in the medium are

436   described by the following equation:

$$Cs = \frac{e^{(-t/\tau)} * Fin,ch * Cs,ch + \left(1 - e^{(-t/\tau)}\right) * Fin,re * Cs,re}{e^{(-t/\tau)} * Fin,ch + \left(1 - e^{(-t/\tau)}\right) * Fin,re}$$

437   In this equation, τ is the time constant for the transition which was set to a value of 16.67 h.

438      $C_{s,ch}$, $C_{s,re}$, $F_{in,ch}$, $F_{in,re}$, correspond to the nutrient concentrations in the chemostat and

439 retentostat media and the feed rates from the corresponding medium reservoirs,

440 respectively. Profiles of the resulting concentrations of the limited nutrient and of glucose in

441 the retentostat feed media during the transition are provided in Supplementary Fig. S3. The

442 actual medium feed rates during the chemostat and retentostat phases for each experiment

443 were calculated from the weight increase of the effluent vessels and the addition rates of

444 base.

Biomass and viability assays

446 Culture dry weight assays were carried out through a filtration, washing and drying

447 procedure as described previously (46). Total cell counts were quantified with a Z2 Coulter

448 counter (50 μm aperture, Beckman, Fullerton, CA). Cell viabilities were determined through

449 a FungaLight™ Yeast CFDA, AM/Propidium Iodide Vitality Kit (a cellular membrane integrity

450 indicator) by flow cytometry and colony-forming-unit counts (6).

Quantification of (by)products and residual substrates

452 Cell-free effluent samples were harvested from a sample port connected to the retentostat

453 filters, immediately frozen in liquid nitrogen and stored at -80 ^{o}C until analysis. Effluent

454 concentrations of glucose, ethanol and by-products (glycerol, lactate, acetate, and succinate)

455 were quantified with HPLC using a Bio-Rad HPX-87H 300 column (7.8 mm). The column was

456 eluted with phosphoric acid (1.5 mM, 0.6 mL/min). The detection was performed with a

457 refractometer (Walters 2414) and a UV dector (Walters 484, 210 nm). Concentrations of

458 ammonium and phosphate were quantified with an ammonium cuvette test (0.02-2.5 mg/L

459 NH_4^+) and a phosphate trace cuvette test (0.03-1.5 mg/L $PO4^{3-}$), respectively (Hach Lange

460 GmbH, Düsseldorf, Germany).

Balances and rate calculations

Biomass-specific glucose and oxygen consumption rates, and biomass-specific production

rates of ethanol, carbon dioxide and by-products were calculated based on primary

measurements of substrates/products concentration and flow rates in gas and liquid phases.

Data reconciliation was performed as described previously (47). The consistencies of the

thus obtained rates were evaluated by calculation of carbon and degree of reduction

recoveries. Ethanol evaporation via the off-gas of the reactor was quantified as described

previously (48) and was taken into account in calculation of ethanol production rates.

Calculation of specific growth rates and doubling times in retentostat cultures was

performed as described previously (4).

Analysis of biomass composition

Around 250 mg of lyophilized biomass was used to determine the elemental (C, H, N, O, P, S)

composition through complete combustion and subsequent gas analysis (carbon dioxide,

water vapour and nitrogen mass fractions), gas chromatography (oxygen) and ICP-MS

(phosphorus and sulphur) (Energy Research Centre, Petten, The Netherlands). Biomass

protein was quantified with the Biuret method as described previously (49). The trehalose

content of the biomass was directly quantified by GC-MS/MS (50) in intracellular metabolite

samples prepared as described below. Glycogen content was quantified through an

enzymatic hydrolysis method (6).

Quantification of intracellular metabolites

A rapid sampling device connected to the bioreactor was used to rapidly withdraw broth

samples for intracellular metabolite measurements (51). Approximately 1.2 g broth was

taken and instantaneously quenched in pre-cooled pure methanol (-40°C), followed by a

484   washing procedure with 80 % aqueous methanol (v/v) solution pre-cooled to -40°C.

485   Metabolite extraction was performed with 75 % (v/v) ethanol (95°C, 3min), followed by

486   rapid vacuum evaporation until dryness. A detailed protocol has been described previously

487   (47). Metabolite concentrations were quantified by isotope dilution mass spectrometry (LC-

488   IDMS/MS and GC-IDMS) using U-^{13}C-labeled yeast cell extract as internal standard (52).

489   Metabolites from glycolysis, TCA cycle and pentose-phosphate pathway as well as amino

490   acids were quantified according to published protocols (53-55). Intracellular adenine

491   nucleotide contents (ATP, ADP, AMP) were measured according to (55). The adenylate

492   Energy Charge(AEC) was calculated as follows:

$$AEC = \frac{ATP + 0.5 * ADP}{ATP + ADP + AMP}$$

493   **Metabolic flux analysis**

494   Intracellular flux distributions during steady-state chemostat and pseudo-steady-state

495   retentostat cultivation were calculated using a slightly modified version of a previously

496   published stoichiometric model (56), in which the biomass composition was adapted

497   according to the measurements of the biomass elemental compositions. The input variables

498   used for the flux analysis are summarized in supplementary Table S3.

503   **Reference**

504   1.   Nielsen J, Keasling JD. 2016. Engineering Cellular Metabolism. Cell 164:1185-1197.
505   2.   Jansen ML, van Gulik WM. 2014. Towards large scale fermentative production of
506   succinic acid. Curr Opin Biotechnol 30:190-197.

507   3.   Ercan O, Bisschops MM, Overkamp W, Jorgensen TR, Ram AF, Smid EJ, Pronk JT,
508   Kuipers OP, Daran-Lapujade P, Kleerebezem M. 2015. Physiological and
509   Transcriptional Responses of Different Industrial Microbes at Near-Zero Specific
510   Growth Rates. Appl Environ Microbiol 81:5662-5670.
511   4.   Boender LG, de Hulster EA, van Maris AJ, Daran-Lapujade PA, Pronk JT. 2009.
512   Quantitative physiology of *Saccharomyces cerevisiae* at near-zero specific growth
513   rates. Appl Environ Microbiol 75:5607-5614.
514   5.   Boender LG, van Maris AJ, de Hulster EA, Almering MJ, van der Klei IJ, Veenhuis M, de
515   Winde JH, Pronk JT, Daran-Lapujade P. 2011. Cellular responses of *Saccharomyces
516   cerevisiae* at near-zero growth rates: transcriptome analysis of anaerobic retentostat
517   cultures. FEMS Yeast Res 11:603-620.
518   6.   Vos T, Hakkaart XD, de Hulster EA, van Maris AJ, Pronk JT, Daran-Lapujade P. 2016.
519   Maintenance-energy requirements and robustness of *Saccharomyces cerevisiae* at
520   aerobic near-zero specific growth rates. Microb Cell Fact 15:111.
521   7.   Bisschops MM, Zwartjens P, Keuter SG, Pronk JT, Daran-Lapujade P. 2014. To divide
522   or not to divide: a key role of Rim15 in calorie-restricted yeast cultures. Biochim
523   Biophys Acta 1843:1020-1030.
524   8.   Pitt SJ. 1982. Maintenance energy: a general model for energy-limited and energy-
525   sufficient growth. Arch Microbiol 133:300-302.
526   9.   Brice C, Cubillos FA, Dequin S, Camarasa C, Martinez C. 2018. Adaptability of the
527   *Saccharomyces cerevisiae* yeasts to wine fermentation conditions relies on their
528   strong ability to consume nitrogen. PLoS One 13:e0192383.
529   10.   Ibstedt S, Stenberg S, Bages S, Gjuvsland AB, Salinas F, Kourtchenko O, Samy JK,
530   Blomberg A, Omholt SW, Liti G, Beltran G, Warringer J. 2015. Concerted evolution of
531   life stage performances signals recent selection on yeast nitrogen use. Mol Biol Evol
532   32:153-161.
533   11.   Taillandier P, Ramon Portugal F, Fuster A, Strehaiano P. 2007. Effect of ammonium
534   concentration on alcoholic fermentation kinetics by wine yeasts for high sugar
535   content. Food Microbiol 24:95-100.
536   12.   Kolouchova I, Matatkova O, Sigler K, Masak J, Rezanka T. 2016. Lipid accumulation by
537   oleaginous and non-oleaginous yeast strains in nitrogen and phosphate limitation.
538   Folia Microbiol (Praha) 61:431-438.
539   13.   Gutteridge A, Pir P, Castrillo JI, Charles PD, Lilley KS, Oliver SG. 2010. Nutrient control
540   of eukaryote cell growth a systems: biology study in yeast. BMC Biology 8.
541   14.   Tai SL, Boer VM, Daran-Lapujade P, Walsh MC, de Winde JH, Daran JM, Pronk JT.
542   2005. Two-dimensional transcriptome analysis in chemostat cultures. Combinatorial
543   effects of oxygen availability and macronutrient limitation in *Saccharomyces
544   cerevisiae*. J Biol Chem 280:437-447.
545   15.   Boer VM, Crutchfield CA, Bradley PH, Botstein D, Rabinowitz JD. 2010. Growth-
546   limiting intracellular metabolites in yeast growing under diverse nutrient limitations.
547   Mol Biol Cell 21:198-211.
548   16.   Boer VM, de Winde JH, Pronk JT, Piper MD. 2003. The genome-wide transcriptional
549   responses of *Saccharomyces cerevisiae* grown on glucose in aerobic chemostat
550   cultures limited for carbon, nitrogen, phosphorus, or sulfur. J Biol Chem 278:3265-
551   3274.

552 17. Ramsay A, Douglas L. 1979. Effects of Phosphate Limitation of Growth on the Cel-
553   Wall and Lipid Composition of *Saccharomyces cerevisiae*. J Gen Microbiol 110:185-
554   191.
555 18. Acquisti C, Kumar S, Elser JJ. 2009. Signatures of nitrogen limitation in the elemental
556   composition of the proteins involved in the metabolic apparatus. Proc Biol Sci
557   276:2605-2610.
558 19. Wada M, Kato J, Chibata I. 1981. Continuous Production of Ethanol in High
559   Concentration Using Immobilized Growthing Yeast Cells. Appl Microbiol Biotechnol
560   11:67-71.
561 20. Taniguchi M, Wakamiya K, Tsuchiya M, Matsuno R, Kamikubo T. 1983. Continuous
562   Ethanol Production by Cell-Holding Culture of Yeasts. Appl Microbiol Biotechnol
563   18:201-206.
564 21. Brandberg T, Gustafsson L, Franzén CJ. 2007. The impact of severe nitrogen limitation
565   and microaerobic conditions on extended continuous cultivations of *Saccharomyces
566   cerevisiae* with cell recirculation. Enzyme Microb Technol 40:585-593.
567 22. De Deken BRH. 1966. The Crabtree Effect: A Regulatory System in Yeast. J gen
568   Microbiol 44:149-156.
569 23. Piper PW. 1995. The heat shock and ethanol stress responses of yeast exhibit
570   extensive similarity and functional overlap. FEMS Microbiol Letters 134:121-127.
571 24. Verduyn C, Postma E, Scheffers W, Dijken Jv. 1990. Energetics of *Saccharomyces
572   cerevisiae* in anaerobic glucose-limited chemostat cultures. J Gen Microbiol 136:405-
573   412.
574 25. Steel CC, Grbin PR, Nichol AW. 2001. The pentose phosphate pathway in the yeasts
575   *Saccharomyces cerevisiae* and *Kloeckera apiculata,* an exercise in comparative
576   metabolism for food and wine science students. Biochem Mol Biol Educ 29:245-249.
577 26. Gournas C, Prévost M, Krammer E-M, André B. 2016. Function and Regulation of
578   Fungal Amino Acid Transporters: Insights from Predicted Structure, p 69-106. *In*
579   Ramos J, Sychrová H, Kschischo M (ed), Yeast Membrane Transport doi:10.1007/978-
580   3-319-25304-6_4. Springer International Publishing, Cham.
581 27. Melnykov AV. 2016. New mechanisms that regulate *Saccharomyces cerevisiae* short
582   peptide transporter achieve balanced intracellular amino acid concentrations. Yeast
583   33:21-31.
584 28. Hazelwood LA, Walsh MC, Luttik MA, Daran-Lapujade P, Pronk JT, Daran JM. 2009.
585   Identity of the growth-limiting nutrient strongly affects storage carbohydrate
586   accumulation in anaerobic chemostat cultures of *Saccharomyces cerevisiae*. Appl
587   Environ Microbiol 75:6876-6885.
588 29. Silljé HHW, Paalman JWG, Schure EGt, Olsthoorn SQB, Verkleij AJ, Boonstra J, Verrips
589   CT. 1999. Function of Trehalose and Glycogen in Cell Cycle Progression and cell
590   viability in *Saccharomyces cerevisiae*. J Bacteriol 181:396-400.
591 30. Petitjean M, Teste MA, Francois JM, Parrou JL. 2015. Yeast Tolerance to Various
592   Stresses Relies on the Trehalose-6P Synthase (Tps1) Protein, Not on Trehalose. J Biol
593   Chem 290:16177-16190.
594 31. De la Fuente IM, Cortes JM, Valero E, Desroches M, Rodrigues S, Malaina I, Martinez
595   L. 2014. On the dynamics of the adenylate energy system: homeorhesis vs
596   homeostasis. PLoS One 9:e108676.
597 32. Gulik WMv, Heijnen JJ. 1995. A metabolic network stoichiometry analysis of microbial
598   growth and product formation. Biotechnol Bioeng 48:681-698.

599   33.   Sonnleitner B, Käppeli O. 1986. Growth of *Saccharomyces cerevisiae* is controlled by
600   its limited respiratory capacity: Formulation and verification of a hypothesis.
601   Biotechnol Bioeng 28:927-937.

602   34.   Pfeiffer T, Schuster S, Bonhoeffer S. 2001. Cooperation and competition in the
603   evolution of ATP-producing pathways. Science 292:504-507.

604   35.   Larsson C, Nilsson A, Blomberg A, Gustafsson L. 1997. Glycolytic flux is conditionally
605   correlated with ATP concentration in *Saccharomyces cerevisiae:* a chemostat study
606   under Carbonor- or Nitrogen-Limiting conditions. J Bacteriol 179:7243-7250.

607   36.   Varela C, Pizarro F, Agosin E. 2004. Biomass content governs fermentation rate in
608   nitrogen-deficient wine musts. Appl Environ Microbiol 70:3392-3400.

609   37.   Larsson C, Stockar Uv, Marison I, Gustafsson L. 1993. Growth and metabolism of
610   *Saccharomyces cerevisiae* in chemostat cultures under carbon, nitrogen, or carbon
611   and nitrogen-limiting conditions. J Bacteriol 175:4809-4816.

612   38.   Lidén G, Persson A, Gustafsson L, Niklasson C. 1995. Energetics and product
613   formation by *Saccharomyces cerevisiae* grown in anaerobic chemostats under
614   nitrogen limitation. Appl Microbiol Biotechnol 43:1034-1038.

615   39.   Cueto-Rojas HF, Milne N, van Helmond W, Pieterse MM, van Maris AJA, Daran JM,
616   Wahl SA. 2017. Membrane potential independent transport of NH3 in the absence of
617   ammonium permeases in *Saccharomyces cerevisiae*. BMC Syst Biol 11:49.

618   40.   Marini A, Soussi-Boudekou S, Vissers S, Andre B. 1997. A family of ammonium
619   transporters in *Saccharomyces cerevisiae*. Mol Cell Biol 17:4282-4293.

620   41.   Ogawa N, DeRisi J, Brown PO. 2000. New Components of a System for Phosphate
621   Accumulation and Polyphosphate Metabolism in *Saccharomyces cerevisiae* Revealed
622   by Genomic Expression Analysis. Mol Biol Cell 11:4309-4321.

623   42.   Gerasimaite R, Mayer A. 2016. Enzymes of yeast polyphosphate metabolism:
624   structure, enzymology and biological roles. Biochem Soc Trans 44:234-9.

625   43.   Borodina I, Nielsen J. 2014. Advances in metabolic engineering of yeast
626   *Saccharomyces cerevisiae* for production of chemicals. Biotechnol J 9:609-20.

627   44.   Nijkamp JF, Broek Mvd, Datema E, Kok Sd, Bosman L, Luttik MA, Daran-Lapujade P,
628   Vongsangnak W, Nielsen J, Heijne WH, Klaassen P, Paddon CJ, Platt D, Kötter P, Ham
629   RCv, Reinders MJ, Pronk JT, Ridder Dd, Daran J-M. 2012. De novo sequencing,
630   assembly and analysis of the genome of the laboratory strain *Saccharomyces*
631   *cerevisiae* CEN.PK113-7D, a model for modern industrial biotechnology. Microb Cell
632   Fact 12.

633   45.   Verduyn C, Postma E, Scheffers WA, Dijken JPV. 1992. Effect of Benzoic Acid on
634   Metabolic Fluxes in Yeasts a continuous culture study on the regulation of respiration
635   and alcoholic fermentation. Yeast 8:501-517.

636   46.   Postma E, Verduyn C, Scheffers WA, Dijken JPV. 1989. Enzymic analysis of the
637   crabtree effect in glucose-limited chemostat cultures of *Saccharomyces cerevisiae*.
638   Appl Environ Microbiol 55:468–477.

639   47.   Lameiras F, Heijnen JJ, van Gulik WM. 2015. Development of tools for quantitative
640   intracellular metabolomics of *Aspergillus niger* chemostat cultures. Metabolomics
641   11:1253-1264.

642   48.   Cueto-Rojas HF, Maleki Seifar R, Ten Pierick A, Heijnen SJ, Wahl A. 2016. Accurate
643   Measurement of the in vivo Ammonium Concentration in *Saccharomyces cerevisiae*.
644   Metabolites 6:1-12.

645   49.   Lange HC, Heijnen JJ. 2001. Statistical reconciliation of the elemental and molecular
646   biomass composition of *Saccharomyces cerevisiae*. Biotechnol Bioeng 75:334-344.
647   50.   Niedenfuhr S, ten Pierick A, van Dam PT, Suarez-Mendez CA, Noh K, Wahl SA. 2016.
648   Natural isotope correction of MS/MS measurements for metabolomics and (13)C
649   fluxomics. Biotechnol Bioeng 113:1137-1147.
650   51.   Lange HC, Eman M, Zuijlen Gv, Visser D, Dam JCv, Frank J, Mattos MJTd, Heijnen JJ.
651   2001. Improved rapid sampling for in vivo kinetics of intracellular metabolites in
652   *Saccharomyces cerevisiae*. Biotechnol Bioeng 75:406-415.
653   52.   Wu L, Mashego MR, van Dam JC, Proell AM, Vinke JL, Ras C, van Winden WA, van
654   Gulik WM, Heijnen JJ. 2005. Quantitative analysis of the microbial metabolome by
655   isotope dilution mass spectrometry using uniformly 13C-labeled cell extracts as
656   internal standards. Anal Biochem 336:164-171.
657   53.   van Dan CJ, Eman RM, Frank J, Lange CH, van Dedem WKG, Heijnen JS. 2002. Analysis
658   of glycolytic intermediates in *Saccharomyces cerevisiae* using anion exchange
659   chromatography and electrospray ionization with tandem mass spectrometric
660   detection. Analytica Chimica Acta 460:209-218.
661   54.   Cipollina C, ten Pierick A, Canelas AB, Seifar RM, van Maris AJ, van Dam JC, Heijnen JJ.
662   2009. A comprehensive method for the quantification of the non-oxidative pentose
663   phosphate pathway intermediates in *Saccharomyces cerevisiae* by GC-IDMS. J
664   Chromatogr B Analyt Technol Biomed Life Sci 877:3231-3236.
665   55.   Seifar RM, Ras C, van Dam JC, van Gulik WM, Heijnen JJ, van Winden WA. 2009.
666   Simultaneous quantification of free nucleotides in complex biological samples using
667   ion pair reversed phase liquid chromatography isotope dilution tandem mass
668   spectrometry. Anal Biochem 388:213-219.
669   56.   Daran-Lapujade P, Jansen ML, Daran JM, van Gulik W, de Winde JH, Pronk JT. 2004.
670   Role of transcriptional regulation in controlling fluxes in central carbon metabolism of
671   *Saccharomyces cerevisiae.* A chemostat culture study. J Biol Chem 279:9125-9138.
672

673

674 **Table 1** Physiological parameters of *S. cerevisiae* CEN.PK113-7D cultured in aerobic

675 ammonium- and phosphate-limited (N- and P-limited) slow growth (SG) (μ = 0.025 h^{-1})

676 steady-state chemostats and near-zero growth (NZG) (μ < 0.002 h^{-1}) pseudo-steady-state

677 retentostats. Data represent averages, with their standard errors, calculated from multiple

678 measurements obtained from duplicate experiments.

Culture condition	Biomass specific net conversion rates								
	$q_{glucose}$[a]	$q_{ethanol}$	q_X	$q_{glycerol}$	$q_{succinate}$	$q_{Lactate}$	$q_{acetate}$	q_{O2}	q_{CO2}
N-limited at SG	14.0 ± 0.0	6.1 ± 0.2	0.96 ± 0.09	0.10 ± 0.01	0.40 ± 0.06	0.070 ± 0.001	0.017 ± 0.002	1.7 ± 0.0	5.5 ± 0.2
P-limited at SG	16.6 ± 1.2	7.9 ± 0.3	0.99 ± 0.04	0.18 ± 0.00	0.15 ± 0.01	0.065 ± 0.001	0.21 ± 0.01	2.1 ± 0.0	6.6 ± 0.3
N-limited at NZG	3.4 ± 0.1	1.5 ± 0.0	---[b]	0.18 ± 0.01	0.30 ± 0.01	0.048 ± 0.002	0.026 ± 0.001	0.71 ± 0.03	1.5 ± 0.0
P-limited at NZG	3.1 ± 0.1	1.1 ± 0.1	---	0.14 ± 0.03	0.15 ± 0.00	0.000 ± 0.000	0.049 ± 0.005	0.94 ± 0.02	1.6 ± 0.1

Culture condition	viability	RQ[c]	Ysx[d]	Ysp[e]	carbon recovery	reduction recovery	Residual nutrient concentrations		
							glucose	NH_4^+	PO_4^{3-}
	%				%	%	g/L	mM	mM
N-limited at SG	93 ± 0	3.1 ± 0.0	0.059 ± 0.000	0.32 ± 0.12	95 ± 1	95 ± 1	16.48 ± 0.2	BD[f]	18.4 ± 0.92
P-limited at SG	91 ± 0	3.1 ± 0.1	0.052 ± 0.000	0.36 ± 0.00	99 ± 6	99 ± 3	18.21 ± 0.7	40.5 ± 2.0	BD
N-limited at NZG	80 ± 0	2.1 ± 0.1	---	0.33 ± 0.02	101 ± 2	98 ± 3	14.99 ± 2.01	BD	18.2 ± 0.90
P-limited at NZG	90 ± 0	1.7 ± 0.0	---	0.28 ± 0.03	98 ± 2	99 ± 1	10.30 ± 0.15	53.5 ± 2.7	BD

679

680

681

682   *a:* Biomass-specific rates were expressed in the unit of $mCmol/g_{xv}/h$, and were calculated

683   based on per gram of viable biomass.

684   *b*: Not calculated.

685   *c:* RQ, respiratory quotient (q_{CO2}/q_{O2}).

686   d: Ysx, Yield of biomass (g biomass/[g glucose consumed]).

687   *e:* Ysp, Yield of ethanol (g ethanol/[g glucose consumed]).

688   *f:* BD, below detection limit of assay.

689

690

691

692

693

694

695

696

697

698

699

700

701

702

703

704

705

706

707

708

709

710 **Table 2** Biomass elemental compositions of *S. cerevisiae* CEN.PK113-7D cultured in aerobic

711 ammonium- and phosphate-limited (N- and P-limited) slow growth (SG) (μ = 0.025 h^{-1})

712 steady-state chemostats and near-zero growth (NZG) (μ < 0.002 h^{-1}) pseudo-steady-state

713 retentostats. Data represent averages, with standard errors, of measurements from

714 duplicate cultures and are compared with published values from aerobic glucose-limited (C-

715 limited) chemostat culture of the same strain (49).

Culture condition	μ	f_C	f_H	f_N	f_O	f_P	f_S	sum	C-mol weight
	h^{-1}	%	%	%	%	%	%	%	g/L
N-limited	0.025	47.0 ± 0.0	7.2 ± 0.0	3.5 ± 0.1	39.5 ± 0.4	1.3 ± 0.0	0.16 ± 0.01	98 ± 0	25.56 ± 0.00
P-limited	0.025	44.0 ± 0.2	7.0 ± 0.1	5.3 ± 0.0	36.9 ± 0.3	0.50 ± 0.01	0.39 ± 0.03	94 ± 0	24.27 ± 0.25
N-limited	< 0.002	49.5 ± 0.4	7.6 ± 0.0	2.5 ± 0.0	39.5 ± 1.1	1.1 ± 0.0	0.11 ± 0.01	100 ± 1	27.33 ± 0.22
P-limited	< 0.002	47.3 ± 0.1	7.2 ± 0.0	4.6 ± 0.1	37.4 ± 0.0	0.29 ± 0.00	0.27 ± 0.01	97 ± 0	25.42 ± 0.08
C-limited	0.022	45.6	6.8	6.6	37.3	1.0	0.22	97	26.4

716
717
718
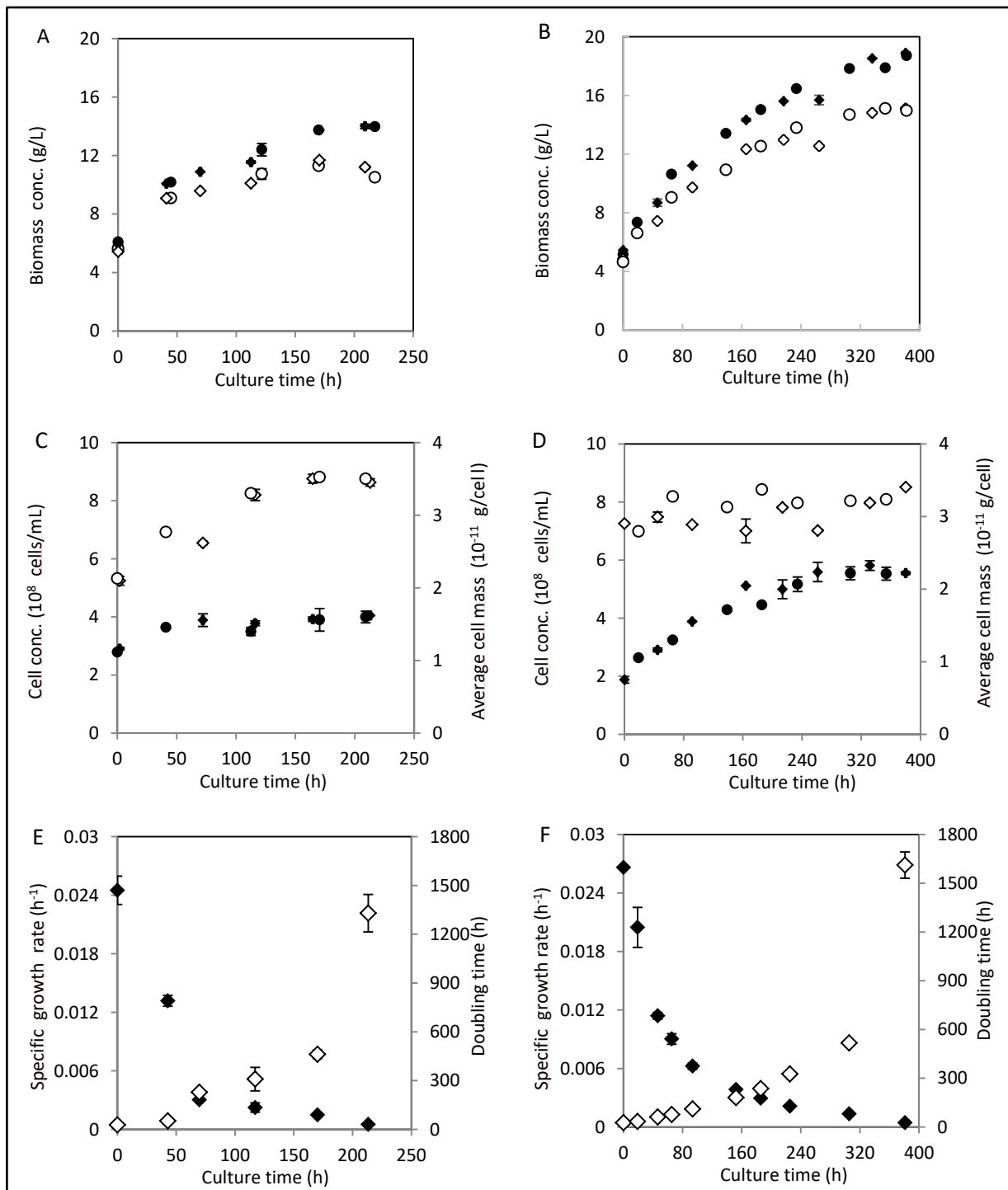719
720
721
722
723
724
725
726
727
728
729
730

Fig. 1 Biomass accumulation, cell counts and specific growth rates in aerobic ammonium- and phosphate-limited retentostat cultures of *S. cerevisiae* CEN.PK113-7D. Data of Fig. 1A, 1B, 1C, and 1D obtained from independent duplicate cultures are shown as circles and diamonds, and error bars indicate standard errors of analytical replicates on samples from the same culture. Data of Fig. 1C and 1D represent the averages and standard errors of measurements on duplicate retentostat cultures.

738   A, B: Total biomass (closed symbols), viable biomass (open symbols) and percentage of

739   viable biomass in ammonium-limited (A) and phosphate-limited (B) retentostat cultures.

740   C, D: Cell numbers (closed symbols) and average mass per cell (open symbols) in

741   ammonium-limited (C) and phosphate-limited (D) retentostat cultures.

742   E, F: Specific growth rate (closed symbols) and doubling time (open symbols) in ammonium-

743   limited (E) and phosphate-limited (F) retentostat cultures.

744

745

746

747

748

749

750

751

752

753

754

755

756

757

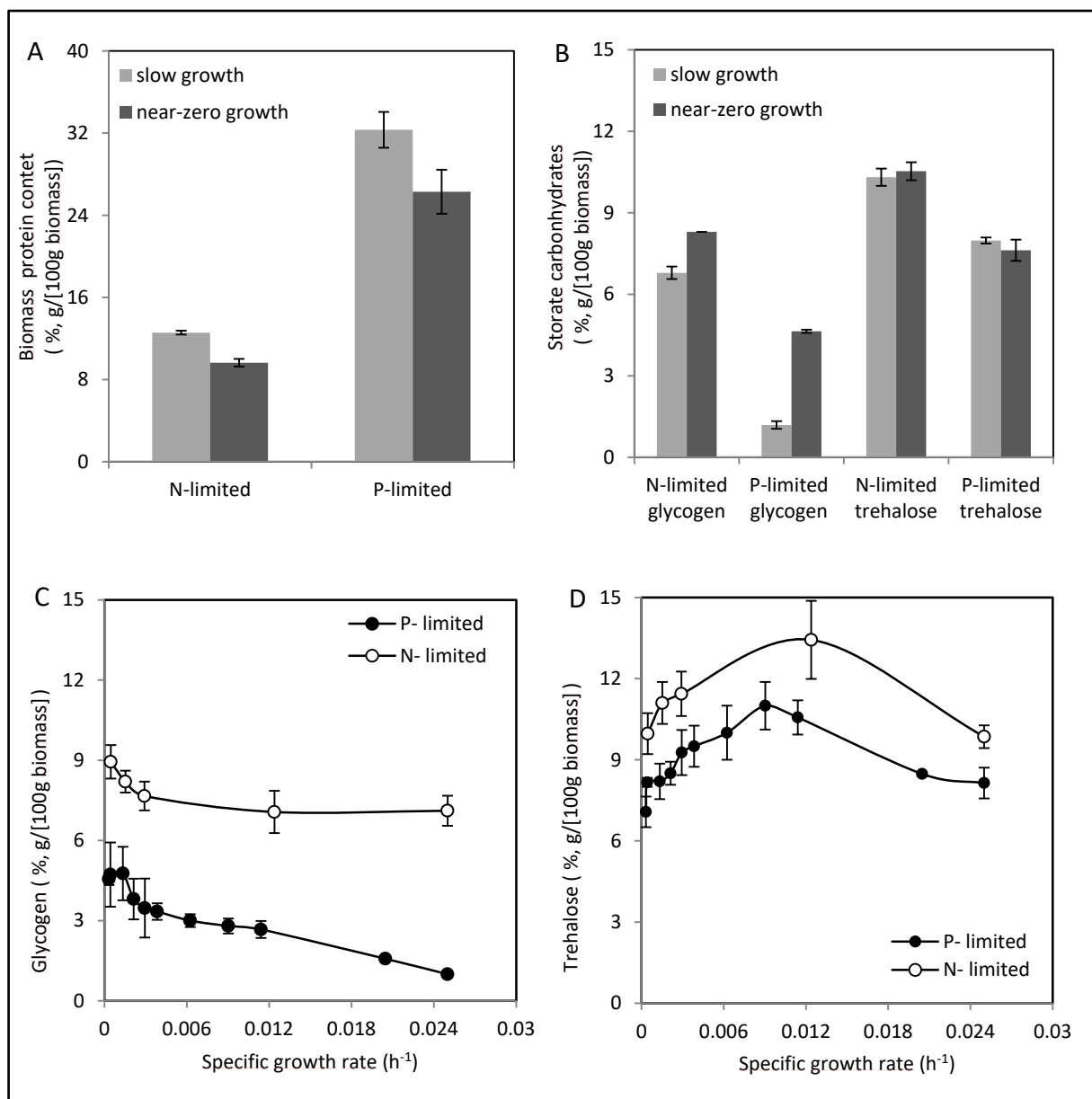758

759

760

761

762

763

764

765

766

767

768

Fig. 2 Biomass protein and storage carbohydrates (glycogen and trehalose) contents in

aerobic ammonium- and phosphate-limited (N- and P-limited) cultures of *S. cerevisiae*

CEN.PK113-7D. Data represent the averages and standard errors of multiple measurements

on duplicate cultures.

A, B: Biomass protein (A) and storage carbohydrates(glycogen and trehalose) (B). Samples

were withdrawn from the steady-state, slow growth ($\mu = 0.025$ h^{-1}) chemostat cultures, and

the pseudo-steady-state, near-zero growth ($\mu < 0.002$ h^{-1}) retentostat cultures.

C, D: Glycogen (C) and trehalose (D) contents vs. the specific growth rate in the prolonged
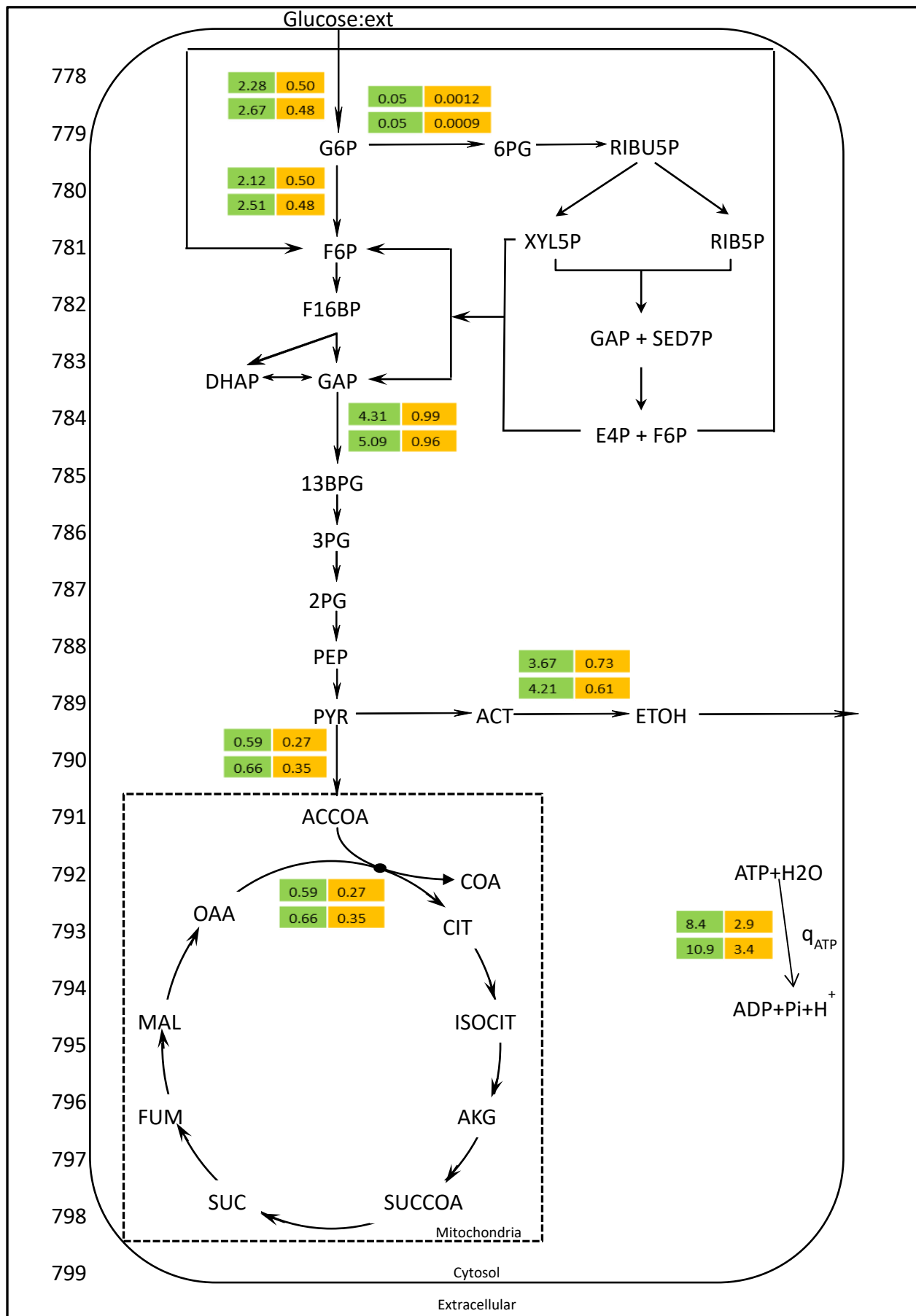
retentostat cultures.

801   **Fig. 3** Metabolic flux analysis in aerobic ammonium- and phosphate-limited (N- and P-

802   limited) cultures of *S. cerevisiae* CEN.PK113-7D. Flux values present the steady-state, slow

803   growth (SG) ($\mu = 0.025$ h^{-1}) chemostat cultures (numbers on green background), and the

804   pseudo-steady-state, near-zero growth (NZG) ($\mu < 0.002$ h^{-1}) retentostat cultures (numbers

805   on orange background). Data are expressed in millmoles of per gram viable biomass per

806   hour and represent the averages of duplicate cultures. Complete flux analysis values and

807   standard errors were presented in Supplementary Table S3.
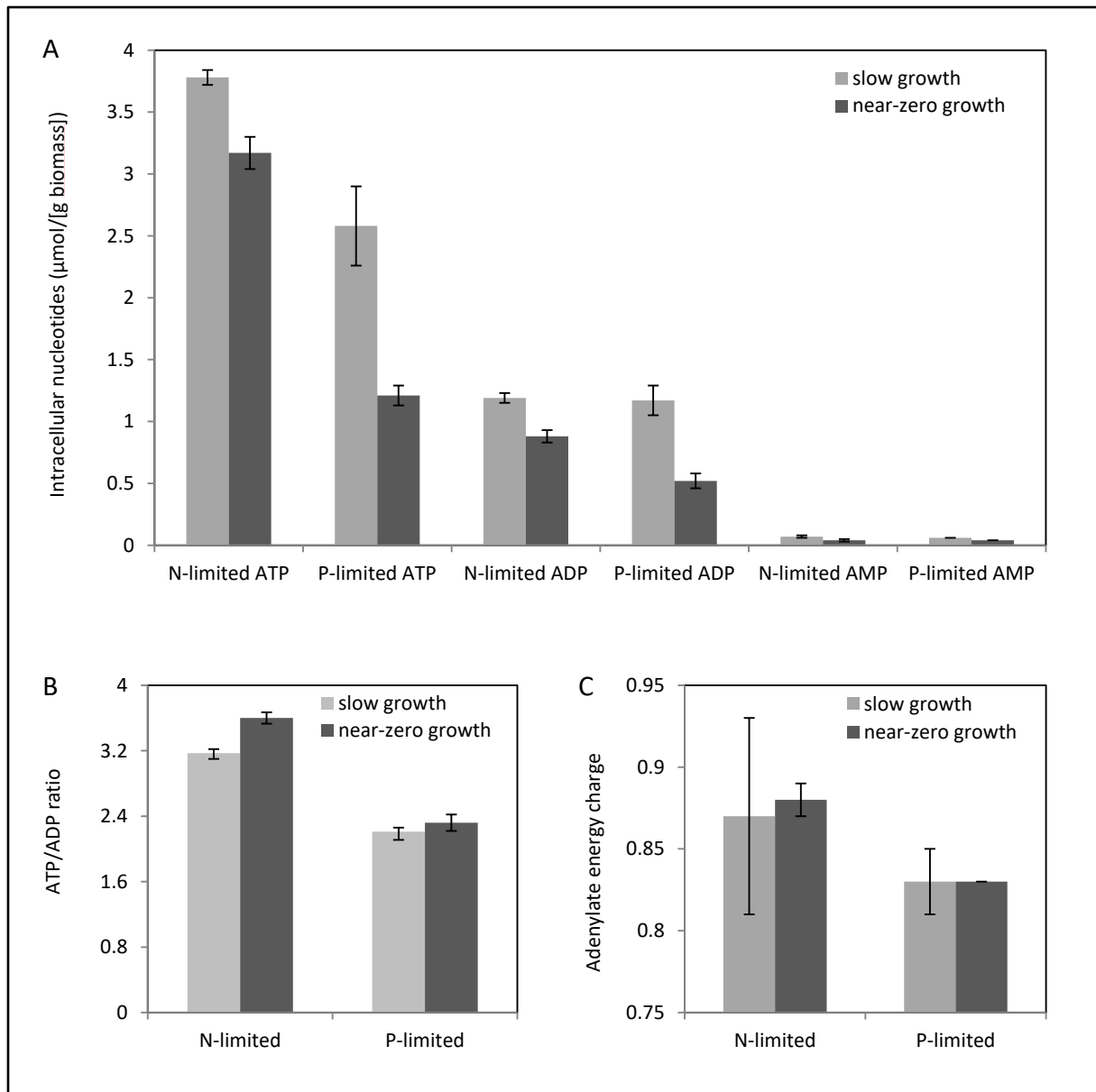
808

809

810

811

812

Fig. 4 Intracellular adenosine phosphate concentrations (3A), ATP/ADP ratio (3B) and energy

charge (3C) in aerobic ammonium- and phosphate-limited (N- and P-limited) cultures of *S.*

cerevisiae CEN.PK113-7D. Data represent the averages and standard errors of multiple

measurements from duplicate cultures. Samples were withdrawn from the steady-state,

slow growth ($\mu = 0.025$ h^{-1}) chemostat cultures, and the pseudo-steady-state, near-zero

growth ($\mu < 0.002$ h^{-1}) retentostat cultures.

819